ACS APPLIED NANO MATERIALS

www.acsanm.org

Forum Article

Antimicrobial and Antioxidant Properties of Photodegraded Amorphous Curcumin on Silica Nanoparticles

Luana Nunes dos Santos Quelé, Mauricio de Matos, Gabriel Goetten de Lima,* Tatiane Brugnari, Carolina Simões Pires Ribeiro, Alessandra Cristina Pedro, Pedro Henrique Gonzalez de Cademartori,* and Washington Luiz Esteves Magalhães

Cite This: https://doi.org/10.1021/acsanm.4c05159

Read Online

ACCESS | Metrics & More | Article Recommendations | Supporting Information

ABSTRACT: This work utilizes the concept of curcumin amorphization to improve drawbacks currently found if it is used as a pharmaceutical ingredient, such as low solubility, limited bioavailability, and absorption, by anchoring it with silica nanoparticles (SiO_2NP). Curcumin loading was determined following kinetic and adsorption parameters, resulting in more than 70% of the curcumin being loaded onto nanoparticles after 180 min. The adjusted data resulted in a Langmuir and BET best-fit with a coefficient relating to favorable adsorption and a multilayer mechanism. With a reduction of more than 70% of the particle area after curcumin loading, it increased the SiO_2NP size. Due to curcumin, FTIR data presented a free unbounded vibration of SiO_2NP, disappearing in favor of a chemical reaction. The XRD pattern showed complete amorphization of curcumin after loading, resulting in a drug release under ethanol of up to 41% in 30 days. To improve this, photodegradation on SiO_2NP with curcumin was performed, showing a vast improvement of the antioxidant activity (ABTS and DPPH) after 72 h, related to the degradation products that were hydrophilic but still lower than pure curcumin, demonstrating the protection effect of SiO_2NP. These led to an increase in antimicrobial potential against fungus and Gram-negative and Gram-positive bacteria when anchored and photodegraded, related to their depolymerization. Docking studies were conducted to assess the antibacterial effect, revealing that the conjugated double bond, a common region for photolysis, remains prominent, even when curcumin is anchored. Interestingly, anchoring curcumin with nanosilica enhances the efficacy, potentially attributed to its antioxidant ability. By anchoring curcumin on nanosilica and performing posterior photolysis, enhanced benefits were achieved by providing support for the degraded products to act in targeted applications such as cancer that can promote stable drug release.

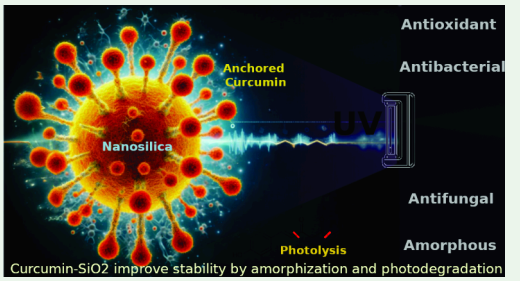

KEYWORDS: *curcumin, amorphization, photodegradation, antimicrobial potential, controlled drug release*

1. INTRODUCTION

Curcumin is a natural compound extracted from the turmeric of *Curcuma longa*. The phenol group in its structure contributes to antioxidant properties, as well as antimicrobial, anticarcinogenic, and anti-inflammatory activity.[1] Due to these unique characteristics, studies have shown that curcumin is considered a potential wound healing agent, in addition to presenting antibacterial properties, essential for the treatment of skin lesions.[2,3]

The anti-inflammatory property of curcumin is attributed to the oxygen free radical scavenger capacity (superoxide, nitric oxide, and hydrogen peroxide), decreasing histamine and cytokine levels. Furthermore, this compound blocks IκK-mediated phosphorylation and IκBα degradation. Thus, nuclear factor (NF)-κB will bind to IκBα and will not induce transcription, an important attribute to consider for impeding constitutive activation and impeding cancer progress.[4,5]

Due to its important and promising properties, curcumin has been used in different industrial segments, such as the textile, food, cosmetic, pharmaceutical, and biomedical fields.[6] However, there are some limitations regarding these actions in the human body, due to the low solubility in the aqueous systems in a body fluid system, which makes it difficult to use in some designs, along with limiting bioavailability and absorption by the body.[7]

This study explores anchoring curcumin, a pharmaceutical ingredient with low solubility, to change its molecular structure and convert it into an amorphous form. By doing this, the drug's release profile can be adjusted: a crystalline form dissolves quickly, while an amorphous form has higher saturation solubility. However, amorphous curcumin is less stable and tends to crystallize over time, especially if stored at

Special Issue: Forum Focused on South American Authors

Received: September 8, 2024
Revised: October 7, 2024
Accepted: October 8, 2024

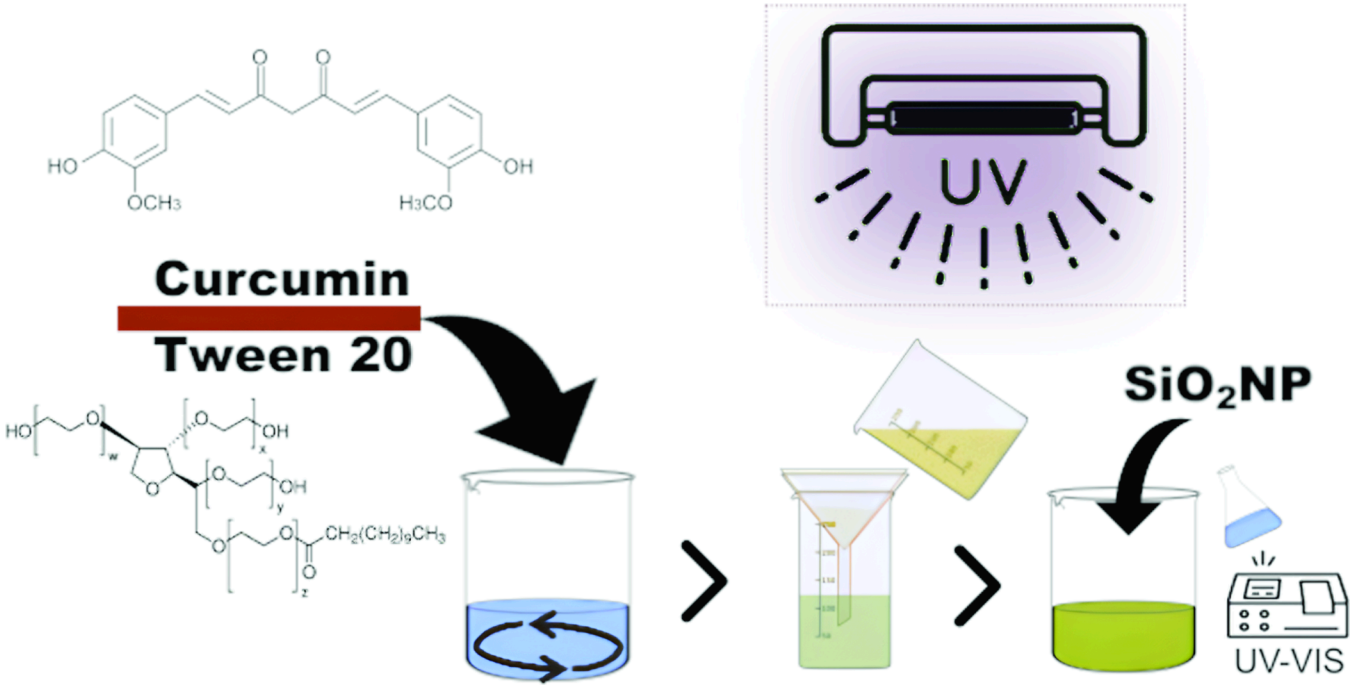

Figure 1. Schematic illustration of curcumin loading onto silica nanoparticles.

temperatures below its glass transition temperature (T_g). This crystallization occurs because the amorphous state is inherently unstable and shifts to a more stable crystalline form upon exposure to such conditions.

Furthermore, utilizing established agents for curcumin encapsulation, such as alginate and pectin, enhances both the protection of curcumin's functionality and its solubility in water. This approach enables the controlled release of curcumin while preserving its biological properties.[8,9] The usage of nanoparticles, in this work nanosilica, for loading curcumin has been widely used in the biomedical field in order to obtain a slow release of active principles, aiming at increasing biological activity in the human body. The usage of silica has been previously reported as a nanocarrier and protector of curcumin, leading to an improvement on the therapeutic effect of cells.[4,10]

Interestingly, studies have shown that the effect of photodegradation on curcumin releases important products, such as vanillin and ferulic acid, that contribute to increasing the solubility of curcumin in aqueous media.[11] Additionally, they provide increased antioxidant activity, decreasing the inflammatory effects of cells.[12] In this context, the objective of this research was to evaluate the effect of the photodegradation of curcumin and the loading of nanosilica with curcumin on the physical and chemical properties, in addition to the antimicrobial and antioxidant potential. This study focuses on the photodegradation of curcumin since these byproducts were shown to promote an enhanced anticancer effect that requires further study when anchored as targeted drug delivery materials.

2. MATERIALS AND METHODS

2.1. Materials. Curcumin, silica nanoparticles (SiO_2NP, CAS no. 112945-52-5), sodium chloride (NaCl), ethyl alcohol, potassium chloride (KCl), 6-hydroxy-2,5,7,8-tetramethylchroman-2-carboxylic acid (Trolox), 2,2′-azino-bis(3-ethylbenzothiazoline-6-sulfonic acid) (ABTS*+), and 2,2-diphenyl-1-picrylhydrazyl (DPPH) were purchased from Sigma-Aldrich (Brazil). Tween 20 (CAS no. 9005-64-5) was purchased from Fagron do Brasil Ltda (Brazil).

2.2. Determination of Curcumin Concentration. For the determination of the curcumin concentration in Tween 20 solution, a curcumin standard calibration curve was constructed. For instance, curcumin solutions were prepared in 1% Tween 20 aqueous solution with a concentration that ranged from 1 to 7 mg L^{-1}. The curve was constructed based on the absorption of each solution in the UV−visible region at a wavelength of 425 nm. A Shimadzu UV-1800 spectrophotometer was used. The 1% Tween 20 solution was used as a blank in the spectrophotometer. Solution concentrations and absorbances for each standard were fitted to a straight line by using linear regression analysis. This produced a model described by the equation $y = 0.1401x - 0.0196$ ($R^2 = 0.9996$), where y is the absorbance and x represents the concentration of the solution.

To determine the concentration of curcumin in ethanol, a calibration curve was constructed with curcumin solutions ranging from 1 to 6 mg L^{-1}. The absorbance reading of each solution was performed at 425 nm. Ethanol was used as a blank in the spectrophotometer. A model described by the equation $y = 0.1622x - 0.0221$ ($R^2 = 0.9965$) was used.

2.3. Loading of Curcumin on SiO_2 Nanoparticles. Curcumin loaded onto SiO_2 nanoparticles (SiO_2NP-CUR) was prepared based on the method proposed by Mattos et al.[13] with modifications. Briefly, 300 mg of curcumin was mixed with 10 mL of Tween 20 for 10 min on a magnetic stir plate at 1500 rpm (Figure 1). Then, 990 mL of DI water was added, and the solution was stirred for another 10 min. Next, the solution was filtered to remove undissolved curcumin, and the curcumin concentration was determined by UV−vis spectrophotometry at 425 nm (~265 mg L^{-1}). Subsequently, 250 mg of SiO_2NP (oven-dried for 3 h at 100 °C) was added to 14 mL of the curcumin solution. The mixture was shaken at 250 rpm in an orbital shaker (I-26 New Brunswick Scientific) at 25 ± 2 °C. Stirring was performed at times of 0, 0.17, 0.33, 0.5, 1, 15, 30, 60, 120, 180, 240, and 300 min. After each time interval, 4 mL aliquots were taken and centrifuged at 10 000 rpm for 10 min, and the concentration of curcumin in the supernatant was determined by UV−vis spectrophotometry at 425 nm. In this way, the amount of adsorbed curcumin q_t (mg g^{-1}) per mass of silica nanoparticles can be calculated at each time (t) of stirring, using eq 1, where C_0 and C_t are the curcumin concentrations (mg L^{-1}) in the solution at the initial time (t_0) and time t,

https://doi.org/10.1021/acsanm.4c05159
ACS Appl. Nano Mater. XXXX, XXX, XXX−XXX

Table 1. Equations for the Determination of Kinetic (Pseudo-First-Order, Pseudo-Second-Order, and Elovich) and Isothermal (Langmuir, Freundlich, and BET) Parameters

model	equation[a]	reference
pseudo-first-order	$q_t = q_1(1 - \exp(k_1 t))$	14
pseudo-second-order	$q_t = \frac{k_2 {q_2}^2 t}{1 + k_2 q_2 t}$	15
Elovich	$q_t = \frac{1}{b}\ln(1 + abt)$	16
Langmuir	$q_e = \frac{q_{max} K_L C_e}{1 + K_L C_e}$	17
Freundlich	$q_t = K_f {C_e}^n$	18
BET	$q_e = \frac{\left[q_{max} K_{BET} \frac{C_e}{1 - C_e}\right][1 - (n+1){C_e}^n + n{C_e}^{n+1}]}{1 + (K_{BET} - 1)C_e - K_{BET}{C_e}^{n+1}}$	19

[a] q_t, adsorption capacity (mg g^{-1}) at time t (min); q_1, theoretical maximum adsorption capacity (mg g^{-1}); k_1, kinetic constant (min^{-1}); q_2, theoretical maximum adsorption capacity (mg g^{-1}); k_2, kinetic constant (mg g^{-1} min^{-1}); a, initial Elovich adsorption rate (mg g^{-1} min^{-1}); b, Elovich desorption rate (mg g^{-1}); q_e, equilibrium adsorption capacity (mg g^{-1}); q_{max}, maximum adsorption capacity (mg g^{-1}); C_e, equilibrium solution concentration (mg g^{-1}); K_L, Langmuir constant (L mg^{-1}); n, constant related to surface heterogeneity; K_f, Freundlich constant (L mg^{-1}); K_{BET}, the BET adsorption constant related to the interaction energy with the surface; and n, the finite number of layers formed.

respectively, m is the mass (g) of the SiO_2NP adsorbent, and V is the volume (L) of the curcumin solution.

$$q_t = \frac{C_0 - C_t}{m} V \quad (1)$$

Recovery of the loaded silica was carried out by centrifugation at 10 000 rpm for 10 min, and the resulting solid was lyophilized (Labconco Freeze-Dry System) at −48 °C for 48 h and dried for another 2 h using a vacuum concentrator (Eppendorf Speed Vac Concentrator Plus). The SiO_2NP-CUR particles were stored in a freezer for further analysis.

The curcumin adsorption isotherm curve on silica was obtained by varying the initial concentration of the curcumin solution (153, 180, 200, 215, 229, 245, 263, 279, 291, 322, and 346 mg L^{-1}). For this, 14 mL of the solution and 250 mg of SiO_2NP were continuously stirred at a constant temperature of 25 ± 2 °C for 3 h to reach reaction equilibrium. After the equilibration time, 4 mL aliquots were taken and analyzed as described above.

The kinetic and adsorption parameters were determined by adjusting the kinetic and adsorption isotherm models listed in Table 1.

2.4. Physicochemical Characterizations. The specific area was determined based on the isotherms of adsorption and desorption of nitrogen (N_2) at 77 K, obtained in a BET equipment model Nova Station A, Quantachrome. The samples were previously dried at 100 °C for 3 h, and the specific surface area (m^2 g^{-1}) was calculated using the Brunauer−Emmett−Teller (BET) multipoint model in the relative pressure range (P/P_0) of 0.05 to 0.35.

Thermogravimetric analyses (TGA) were performed using DTG-60H Shimadzu equipment with a N_2 flow of 50 mL min^{-1}, a temperature range of 30−600 °C, and a heating rate of 10 °C min^{-1}. The initial mass of the samples ranged from 5 to 10 mg. Alumina crucibles were used.

Fourier transform mid-infrared (FTIR) spectra were collected on a Thermo Scientific Nicolet iS50 spectrophotometer in absorbance mode, in the range of 4000 to 400 cm^{-1}, with a resolution of 2 cm^{-1} and 64 scans. Samples were prepared in KBr tables at a concentration of 0.1 (wt %).

Scanning electron microscopy (SEM) was performed for SEM analysis with a HITACHI model TM3000 instrument operating at 15 kV.

XRD analysis was performed on a Bruker D2 Phaser diffractometer, using Cu Kα radiation, an angular range from 10° to 90°, a step of 0.02°, and 0.8 s per step.

2.5. In Vitro Release Studies. To study the release of curcumin from the charged particles (SiO_2NP-CUR), 1 g of the charged silica particles was added to 25 mL of two different solvents (1% Tween 20 solution and ethanol) under agitation at 250 rpm without exposure to light sources and with room temperature control at 30 °C. At time intervals of 0, 2, 4, 20, 24, 42, 48, and 720 h, a 4 mL aliquot of each solution was removed, centrifuged, and analyzed by UV−vis spectrophotometry at a wavelength of 425 nm. After analysis, the aliquots were returned to the reaction medium. The cumulative release of curcumin (CR%) was determined by eq 2, where C_0 is the mass of curcumin contained in the particles divided by the volume of the various media used in the release and C_t is the concentration of curcumin in the solution after each sampling time.

$$CR\% = \frac{C_t}{C_0} \times 100 \quad (2)$$

2.6. Photodegradation Studies. For the study of curcumin degradation when exposed to visible light, 1 g of curcumin loaded onto SiO_2 nanoparticles (SiO_2NP-CUR), 14.8 mg of curcumin (CUR), and 14.8 mg of curcumin with 250 μL of Tween 20 (CUR-T20) were added, separately, to 25 mL of distilled water under stirring at 150 rpm with exposure to a light source. The distance from the sample to the lamp was 10 cm. The experiment was carried out at a temperature of 25 ± 2 °C and maintained for 72 h. After the reaction time, the samples were dried in a freeze-drier for 48 h and stored for further analysis.

2.7. Antioxidant Capacity. Antioxidant activity was determined by 2,2′-azino-bis(3-ethylbenzothiazoline-6-sulfonic acid) (ABTS) and 2,2-diphenyl-1-picrylhydrazyl (DPPH) radical assay in vitro assays. Standard curves for all assays were prepared with Trolox, and results are expressed in mole of Trolox equivalent per gram of dry weight of sample (molTEAC/g).

The ABTS radical cation decolonization assay was determined according to the method of Re and Rufino.[20,21] The working solution was prepared by mixing 5 mL of 7 mmol/L ABTS and 88 μL of 140 mmol/L potassium persulfate and allowing them to react for 16 h at room temperature (25 ± 2 °C) in the dark. The solution was diluted by mixing 1 mL of ABTS radical solution with 50 mL of ethanol to obtain an absorbance of 1.10 at 734 nm. A total of 990 μL of an ABTS solution and 10 μL of diluted extract were added to 1 mL test tubes. The mixture was stored in the dark for 2 h and then the absorbance was measured at 734 nm.

The ability of extracts to scavenge the DPPH· was determined according to the method of Brand-Williams et al.[22] First, 550 μL of

https://doi.org/10.1021/acsanm.4c05159
ACS Appl. Nano Mater. XXXX, XXX, XXX−XXX

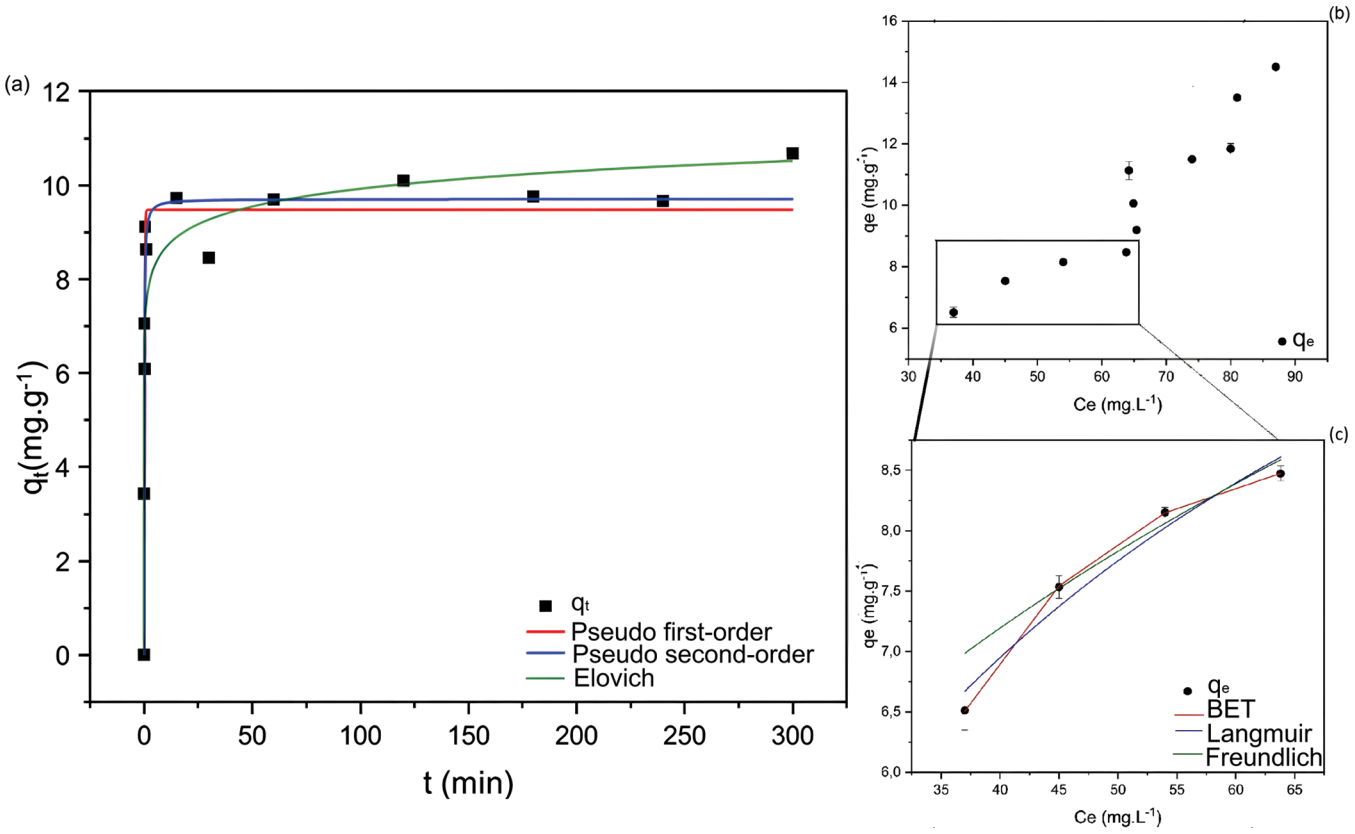

Figure 2. (a) Adsorption kinetic curves of curcumin on silica nanoparticles, fitted to pseudo-first-order, pseudo-second-order, and Elovich models. Adsorption was carried out at 25 ± 2 °C and 250 rpm, with a curcumin concentration of 265 mg L^{-1}. (b) Curcumin adsorption isotherm. (c) Adjustments of the BET, Langmuir, and Freundlich isothermal models within the first adsorption layer.

ethanol and 350 μL of a 223 μmol/L methanol DPPH solution were added to 1 mL test tubes. The mixture was stored in the dark for 30 min and then the absorbance was determined at 517 nm.

2.8. Antimicrobial Potential of Curcumin. The susceptibility of microorganisms *Aspergillus niger*, *Trichoderma* sp. (isolated and identified macro and micromorphologically in the Biotechnology Laboratory of UTFPR), *Escherichia coli* (ATCC25922), and *Staphylococcus aureus* (ATCC6538) was studied. Samples of curcumin and photodegraded curcumin were analyzed by the broth microdilution method, as provided for by Clinical and Laboratory Standards Institute (CLSI/NCCLS): M7-A6 for bacteria and M38-A for filamentous fungi.

The bacteria were previously cultured on Mueller−Hinton agar for 24 h at 35 °C, and the fungi were cultivated on potato dextrose medium for 7 days at 28 °C. For the test, 96-well microplates were used, containing 50 μL of each sample previously diluted, by serial methodology, in Mueller−Hinton medium for bacteria and Sabouraud medium for fungi. Then, 50 μL of freshly prepared microbial inoculum at specific concentrations was added to all wells in order to obtain final concentrations of 5×10^5 CFU mL^{-1} for bacteria and 5×10^4 CFU mL^{-1} for fungi. The microplates were incubated at 28 °C for filamentous fungi and 35 °C for bacteria, both for 48 and 24 h, respectively.

The antimicrobial potential of the samples was then verified by the turbidity of the reaction medium, analyzed in a spectrophotometer (625 nm for bacteria and 530 nm for fungi), and expressed as a percentage of reduction in the growth of microorganisms in relation to the microbial growth control (culture medium containing only the microorganism). The same procedure was performed using autoclaved distilled water as a negative control and, as positive controls, amoxicillin standard for *S. aureus* bacteria (1 μg mL^{-1}), trimethoprim (20 μg mL^{-1}) for *E. coli*, and cycloheximide (50 μg mL^{-1}) for fungi. All analyses were performed in triplicate.

2.9. Preprocessing of Molecules Prior to Simulation. The 3D structures of curcumin and its derivatives were built using MarvinSketch and checked against tautomers. Then with Avogadro software, the energy was optimized, and a conformer random search was performed using the MMF94 force field with the energy being minimized. The semi-empirical PM7 method was also used to optimize the geometry with MOPAC2016 software.[23]

For fumed silica, the molecule builder was performed using the interface force field, interface_ff,[24] that matches the specifics from the commercial product, with a size of <200 nm, an area density of the silanol groups of 4.7 per nm^2, with no (SiO^- M^+) per nm^2.

2.10. Docking Simulation. The docking methodology was first prepared by using AutoDockTools[25] in order to start docking the input files. Protein was transformed from *.pdb files to *.pdbqt, where the heteroatoms and alternates were removed and protonation states were added while also merging charges and removing nonpolar hydrogens. For ligand, protonation states were added, charges were merged, and nonpolar hydrogens were removed using pH 7.4[26] with the AMBER Force Field. A search space was defined, blind docking.

Docking was then performed using the AutoDock Vina tool with 4 CPU usages, an exhaustiveness of 16, and 20 number of modes, repeating the run 10 times. For the docking with silica, the HEX 8.0.0[27] software was used with a 3D FFT mode using a final search of 30 steps and a steric scan.

3. RESULTS AND DISCUSSION

3.1. Loading of Curcumin on SiO_2 Nanoparticles. The kinetic study was carried out with the objective of evaluating the affinity between the adsorbent and the adsorbate in addition to establishing the equilibrium time. The kinetic data show that the adsorption is faster in the first 10 min, probably due to the greater availability of adsorption sites available on

https://doi.org/10.1021/acsanm.4c05159
ACS Appl. Nano Mater. XXXX, XXX, XXX−XXX

the surface of SiO_2NP.[28] Figure 2a exhibits that after 300 min, approximately 72% of the curcumin present in the solution was loaded onto the nanoparticles (about 10.5 mg g^{-1}).

As shown in Figure 2, the adsorptive process becomes slower over time, probably due to the difficulty in occupying the remaining vacant sites and the reduction in the concentration of curcumin in the solution. Apparently, the adsorption of curcumin on the silica surface is more energetically favorable when compared to the adsorption on previously adsorbed curcumin molecules. Reaction equilibrium is reached when the activity of curcumin dissolved in the solution equals the activity of curcumin adsorbed on the surface of silica nanoparticles.[29] The adsorption process reached kinetic equilibrium at around 120 min, showing removal of approximately 67% of curcumin from the solution. Therefore, the stirring time was optimized to 180 min for subsequent experiments to ensure that an equilibrium was reached.

The adsorption process best-fit relates to the pseudo-second-order model, judging by the comparison of the coefficients of determination (R^2) (Table 2). This model describes that the rate limiting step of adsorption can be characterized by a chemical sorption involving valence forces, through the sharing or exchange of electrons between the adsorbent and the adsorbate.[30,31]

Table 2. Kinetic Parameters Obtained from the Adjustments of the Adsorption Data of Curcumin on Silica Nanoparticles by the Elovich, Pseudo-Second-Order, and Pseudo-First-Order Models and Isothermal Parameters Obtained from the Adjustments to the Langmuir, Freundlich, and BET Models in the Kinetic Equilibrium in the First Adsorption Layer[a]

model	R^2	parameter	
Elovich	0.82	q_e (mg g^{-1})	$(4 \pm 1) \times 10^6$
		k (mg g^{-1})	1.8 ± 0.4
pseudo-second-order	0.94	k_2 (mg g^{-1} min^{-1})	1.1 ± 0.3
		q_e (mg g^{-1})	9.7 ± 0.3
pseudo-first-order	0.91	q_e (mg g^{-1})	9.5 ± 0.3
		k_1 (min^{-1})	6.0 ± 1.3
Langmuir	0.96	q_{max} (mg g^{-1})	14 ± 2
		K_L (L mg^{-1})	0.02 ± 0.01
Freundlich	0.77	n_f	0.38 ± 0.09
		K_f (L mg^{-1})	1.8 ± 0.7
BET	0.99	q_{max} (mg g^{-1})	8.9 ± 0.04
		K_{BET}	$(5 \pm 2) \times 10^{-6}$
		n	3.7 ± 0.1

[a]Kinetic models: q_e, maximum theoretical adsorption capacity; k_1, kinetic constant; k_2, kinetic constant (mg g^{-1} min^{-1}); q_e, initial Elovich adsorption rate (mg g^{-1}); and k, Elovich desorption rate (mg g^{-1}). Isothermal models: q_{max}, maximum adsorption capacity; C_e, concentration of the solution at equilibrium (mg g^{-1}); K_L, Langmuir constant; n_f, constant related to surface heterogeneity; K_f, Freundlich constant (L mg^{-1}); K_{BET}, BET adsorption constant related to surface interaction energy; and n, the finite number of layers formed.

The adsorption isotherm (Figure 2b) shows a sigmoidal curve with the presence of an inflection point and more than one plateau, which may indicate a type S isotherm with a type 4 subgroup, suggesting that at least two opposing mechanisms may occur. According to Giles et al.,[32] such isotherms have two causes. The first refers to the attractive solute−solute forces on the surface that can cause cooperative adsorption, and the second refers to the sorption of a solute that can be inhibited through a competitive reaction within the solution.

To evaluate the curcumin adsorption mechanism on SiO_2NP, Langmuir, Freundlich, and BET models were used. The Langmuir model is known as a monolayer adsorption, in which the adsorbent surface is assumed to be homogeneous, and each surface site is occupied by only one adsorbate molecule. From the Langmuir constant (K_L), the separation factor (R_L) is obtained and indicates whether the adsorption process is favorable or unfavorable. For the isotherm of the adsorption of curcumin on SiO_2NP, the R_L was 0.012, which indicates that the process is favorable since the R_L is between 0 and 1. R_L equal to 1 indicates an irreversible process, and values greater than 1 indicate an unfavorable process.[33] The Freundlich model describes multilayer adsorption, where the adsorbent has an unlimited number of adsorptive sites on the surface, and the adsorption mechanism is heterogeneous. From parameter n of the Freundlich model, information about the heterogeneity of the adsorbent surface can be obtained. In this study, the value of n was approximately 0.5 (Table 2), and as $n < 1$, the adsorption process is considered favorable.[33] From the data of the adsorption isotherm and the parameters obtained by adjustments with the models, it is observed that the best-fit model for the adsorption curve of curcumin on SiO_2NP is the BET model. This model describes multilayer adsorption. According to their basic hypotheses, a site can bind many molecules, considering that the first one constitutes a new receptor site for the subsequent one.[34] These positive results are even more attractive since it remains as a stable structure after curcumin anchoring (Supporting Information, Figure S1).

3.2. Physicochemical Characterizations. The SiO_2NP-CUR N_2 adsorption and desorption isotherms (Figure 3a) can be classified according to the International Union of Pure and Applied Chemistry (IUPAC) as type IV, as they have a hysteresis loop. The shape of the hysteresis is mainly determined by the pore geometry. Thus, the isotherm of the analyzed sample is of the H3 type, common for adsorption in aggregate structures formed from connected pores.[35] The specific area calculated using the BET model (Figure 3b) shows that there was a reduction of more than 70% of the particle area after curcumin loading, when compared to the unloaded silica particles. The decrease in specific area may be related to an increase in the size of the silica particles after loading with curcumin, indicating that the dimensions were changed due to the adsorption of curcumin on the silica active sites of the particles in more than one layer. Similar results were obtained when loading SiO_2NP with neem oil.[36]

The thermal degradation of the analyzed pure and anchored curcumin (Figure 3c,d) presents typical behavior, in which curcumin degradation occurs in two steps, one around 250−400 °C (Figure 3c) and another at 400−600 °C with the formation of residual matter. Tween presented a degradation profile around 300−440 °C with a peak at ∼412 °C (Figure 2c). Silica nanoparticles are known to be a very stable material presenting a small weight loss based on condensation of silica groups; the degradation pattern seen from 300 to 600 °C is due to the Tween addition.

However, when curcumin is added, a small decrease in degradation is seen; this can be related to SiO_2NP, which has been reported to exert a stabilizing effect on loaded compounds. Therefore, there is an increase in thermal stability of curcumin related to a chemical reaction between curcumin and silica nanoparticles; also, the small variation in DTA

https://doi.org/10.1021/acsanm.4c05159
ACS Appl. Nano Mater. XXXX, XXX, XXX−XXX

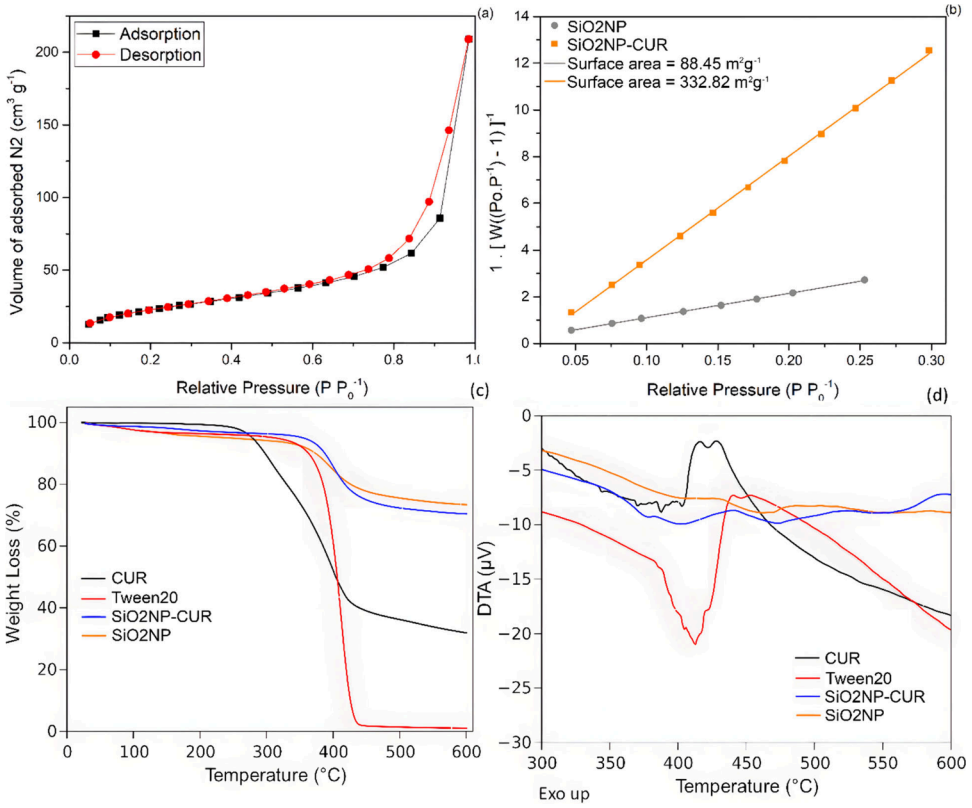

Figure 3. (a) Adsorption and desorption isotherms of nitrogen at 77 K under curcumin-loaded silica nanoparticles. (b) Linearization of isotherms using the BET model for determination of surface areas for silica nanoparticles with and without curcumin. (c) Thermogravimetric analysis and (d) differential thermal analysis for pure compounds and anchored curcumin.

(Figure 3d) could indicate that the curcumin is in an amorphous state, and what is seen is the result of Tween. Pure curcumin typically exhibits a characteristic degradation profile. However, when encapsulated in silica, curcumin remained relatively stable, suggesting that silica not only delays its melting but also provides thermal protection, a well-documented effect.

After curcumin was anchored to silica nanoparticles, changes were observed in the FTIR spectra (Figure 4a) that are not due to just a linear combination of the spectra of silica and curcumin. A decrease in the intensity, displacement, and modification of the appearance of the bands referring to water and OH in the nanoparticles in the region between 3730 and 3000 cm^{-1} is seen. An important band referring to water on the silica surface in the region at around 1642 cm^{-1} disappears completely after the adsorption of curcumin on the particles. A new band is observed at 1351 cm^{-1}, which is related to aromatic unsaturation (C═C) for pure curcumin, so in this case, the loading of curcumin led to favorable chemical bonds.

In the silica particles, some organic impurities are already visible in the spectrum and remain stable. Finally, the other major change is the band shift from 967 to 948 cm^{-1} after curcumin adsorption. These modifications corroborate the second-order adsorption model, which suggests the chemical reaction of curcumin on silica nanoparticles. This probably occurs with the reaction between the phenolic OH of curcumin and the hydroxyls of the silica surface. This explains the modification of the vibrational region of OH groups with intensity reduction and signal displacement, as well as the increase in intensity in the region of CH and CH_2.

Since there is a chemical reaction occurring between curcumin and SiO_2NP, this affects the chain ordering. As seen by the XRD results (Figure 4b), the crystalline curcumin becomes amorphous with a very wide peak within the region of this compound's peaks. The effect of the nanoencapsulation operation reduces the curcumin particle size and changes the nature of the drug, referred to as the amorphization process.[37]

3.3. In Vitro Release. Because curcumin has low solubility in water, we decided to carry out release experiments in solvents in which curcumin is more soluble. Ethanol and a 1% Tween 20 aqueous solution were used. In both solvents used, there was a burst release as soon as the particles came into contact with the solvents (Figure 4c). When the solvent used was ethanol, the release of curcumin from the samples proceeded slowly, not exceeding a maximum of approximately 41% in 30 days (Figure 4c). This result corroborates the kinetic model of adsorption (pseudo-second-order), which suggests a chemical reaction between curcumin and the surface of silica nanoparticles. As the chemical reaction occurs only in the first layer, the release must occur by removing curcumin from the other adsorbed layers. A simple mass balance shows that the percentage not released (~59%) equates to about 8.8 mg g^{-1}, a value that is very close to the maximum concentration found in the adsorption isotherm of the first layer (~8.5 mg g^{-1}).

As for the samples released in aqueous medium with the addition of 1% Tween 20, it was observed that there was a burst release of 15.8%. Subsequently, the concentration released decreased continuously, probably due to some precipitation or resorption of curcumin after release into the aqueous medium. Due to the synthesized silica organization, it

https://doi.org/10.1021/acsanm.4c05159
ACS Appl. Nano Mater. XXXX, XXX, XXX−XXX

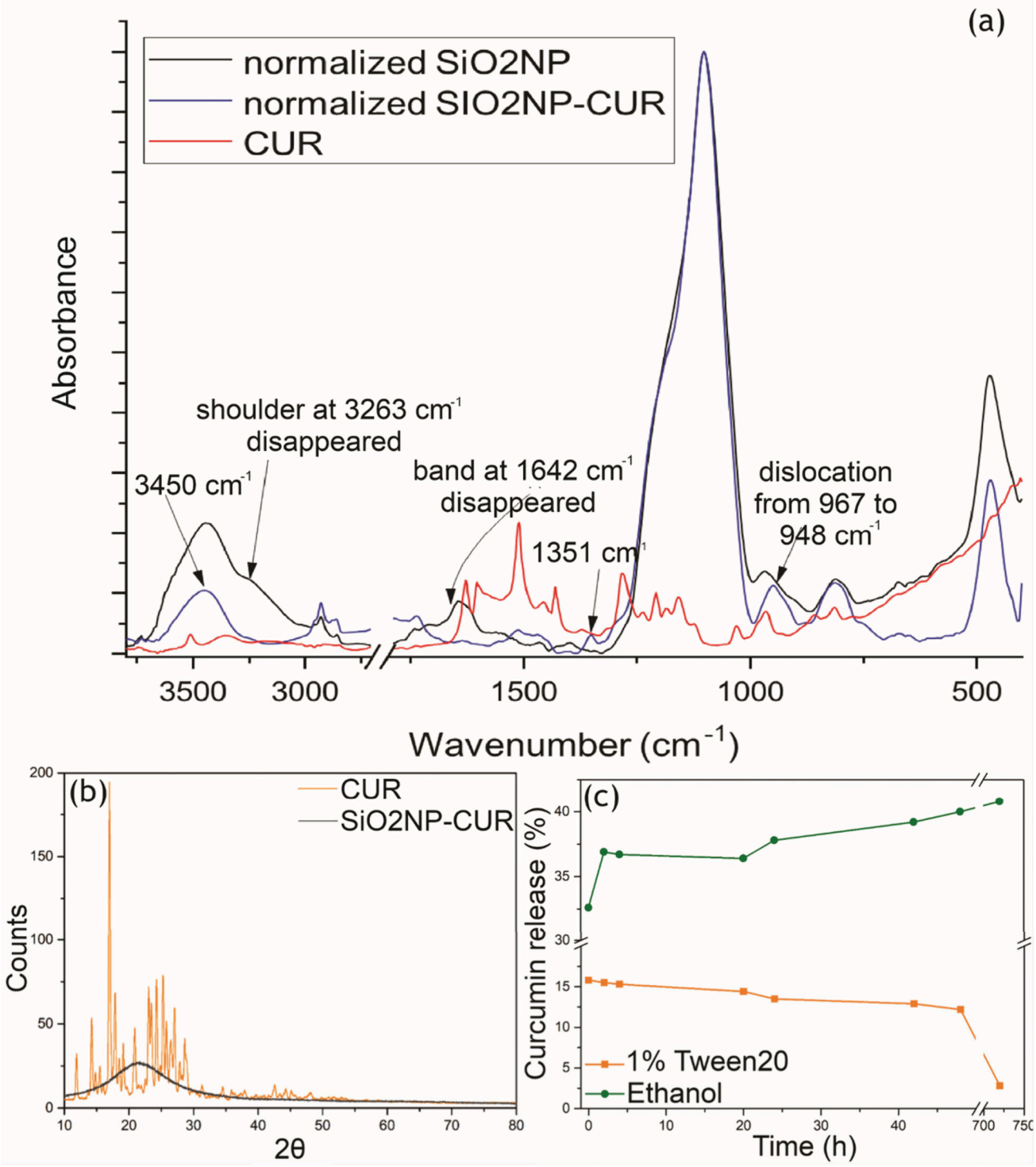

Figure 4. (a) FTIR spectra of samples of silica nanoparticles loaded with (SiO_2NP-CUR) and without curcumin (SiO_2NP) after being divided by the intensity of the highest peak (normalization). Also shown is the spectrum of pure curcumin. (b) X-ray diffraction profiles for pure curcumin and curcumin loaded onto SiO_2NP. (c) Drug release studies of SiO_2NP-CUR.

is possible to anchor drugs and stabilize them as amorphous, which increases the drug dissolution rate.

3.4. Photodegradation. The effect of photodegradation on thermal stability exhibits that an increased, sharper endotherm area peak occurs for curcumin loaded on Tween 20 (Figure 5a). This indicates that photodegradation, besides exposing the chemical bonds and chain reordering, may have induced a stiffer structure with non-loose bounds (Figure 5b). Therefore, since the degradation occurs in a shorter temperature range, it indicates a chemical interaction. Nonetheless, photodegradation of anchored curcumin on SiO_2NP presents a different profile, with the thermal degradation starting earlier and with a broad and wider endothermic peak. It is possible that the chemical reactions seen for pure curcumin with nanosilica may have altered to a state of weaker bonds due to

https://doi.org/10.1021/acsanm.4c05159
ACS Appl. Nano Mater. XXXX, XXX, XXX−XXX

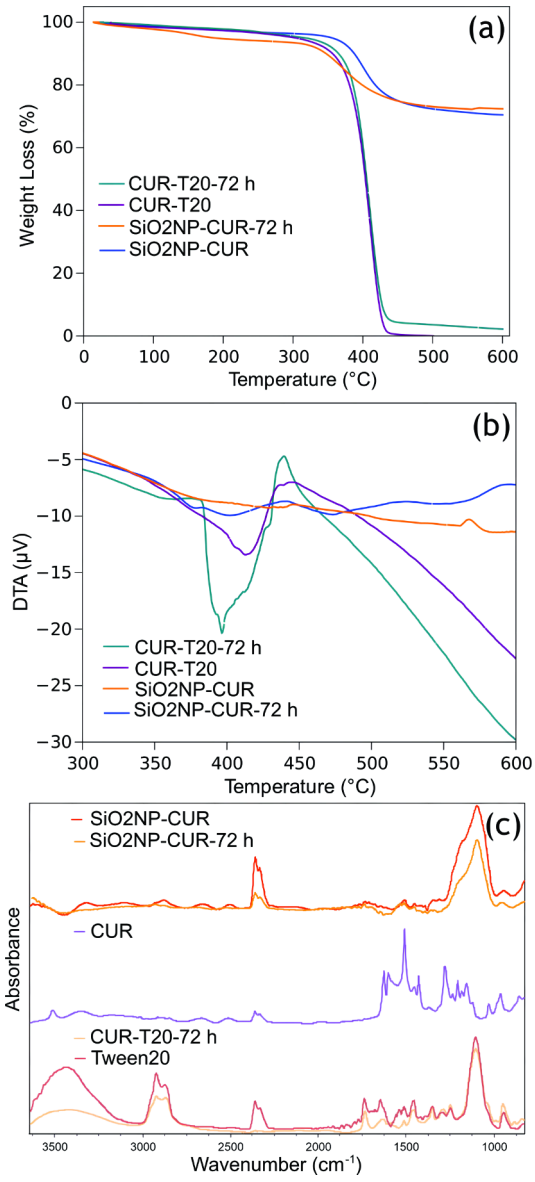

Figure 5. (a) Thermogravimetric analysis and (b) differential thermal analysis for pure compounds and anchored curcumin before and after photodegradation. (c) FTIR spectra of the studied samples before and after photodegradation of curcumin at 72 h.

the irradiation intensity, altering the molecular arrangements of intermolecular bonds from curcumin.

The thermal stability seen for the curcumin loaded onto Tween and nanosilica can be better explained by the FTIR spectra (Figure 5c), in which the photodegradation causes a decreased intensity of the bands assigned to nanosilica and Tween. However, bands attributed to curcumin appeared to present the same intensity after photodegradation and, in some cases, even increased in intensity, as is the case with the bands at 1511 and 950 cm^{-1}. Additionally, there was a heavy reduction of the OH groups after photodegradation with a slight reduction of the hydroxyls of silica, also indicating that free unbound water is given preference for disassociating of bonds in favor of curcumin.

It is possible that the photodegradation of curcumin within the silica matrix may have weakened some of the molecular bonds; yet, the overall structure exhibited minimal deviations in DTA values. This indicates that these weakened bonds may have interacted with silica, leading to stabilization. In contrast, curcumin combined with Tween displayed significant peaks and valleys in DTA, corresponding to the degradation temperature observed in the TGA analysis.

3.5. Antioxidant Activity of Curcumin. Curcumin is a phenolic compound widely used as a commercial dietary supplement and additive due to its promising antioxidant effects. Studies have demonstrated its important effects on chronic diseases such as inflammation, cancer, diabetes, cardiovascular, neurological, and pulmonary diseases.[38] However, the biomedical and pharmaceutical application of curcumin has been hampered due to its malabsorption, water insolubility, accelerated metabolism, spontaneous oxidative degradation, and low bioavailability.[39] Thus, the antioxidant action of this compound in human tissue is weak, hindering the biological properties attributed to curcumin.

Nanotechnology based strategies for slow and targeted drug delivery are being developed to overcome the aforementioned difficulties. In this context, silica nanoparticles have been applied as hydrophilic carrier systems to cross barriers and internalize cells in biomedical, food, and pharmaceutical applications.[40] With this objective, our study was based on the loading of silica with curcumin diluted in Tween 20, for a slow and controlled release of curcumin. In addition, the degradation of the samples was performed, and the antioxidant activity by the ABTS and DPPH methods was determined, as shown in Table 3.

Table 3. Antioxidant Activity of Curcumin Samples with and without Degradation

sample	ABTS (mol g^{-1})	DPPH (mol g^{-1})
curcumin (0 h)	2.2443 ± 0.0066	0.4409 ± 0.0020
curcumin (72 h)	9.0197 ± 0.0001	8.2719 ± 0.0084
CUR-T20 (0 h)	0.0003 ± 0.0001	0.0002 ± 0.0001
CUR-T20 (72 h)	0.0013 ± 0.0001	0.0010 ± 0.0001
SiO_2NP-CUR (72 h)	0.0072 ± 0.0002	0.0076 ± 0.0001

As shown in Table 3, the process of photodegradation of curcumin for a period of 72 h showed increased antioxidant activity by the ABTS and DPPH methods when compared to the nondegraded samples (0 h). Furthermore, it is observed that nondegraded (2.2443 and 0.4409 mol g^{-1}) and degraded (9.0197 and 8.2719 mol g^{-1}) free curcumin showed higher values of antioxidant activity compared to samples with Tween 20 and silica. In 2021, Jung and Hong[41] showed that the degradation of in natura curcumin by the irradiation process for 24 h also provided an increase in antioxidant activity by the ABTS method, by about 15−19% in relation to the nondegraded sample, suggesting that products derived from curcuminoids possess considerable antioxidant activities.

The degradation of curcumin occurs through the cleavage of the β-diketone bond, forming hydrophilic and lower molecular weight phenolic compounds, such as ferulic acid, feruloyl methane, vanillic acid, vanillin, *p*-hydroxybenzoic acid, and *p*-hydroxybenzaldehyde.[42] These degradation products are hydrophilic, unlike in natura curcumin, which is hydrophobic in nature. Thus, the antioxidant potential of curcumin photodegradation products tends to present greater antioxidant activity in the ABTS assay, as it is an aqueous system. Conversely, in the DPPH method, they may be less effective, as the solution is prepared using methanol.[43]

https://doi.org/10.1021/acsanm.4c05159
ACS Appl. Nano Mater. XXXX, XXX, XXX−XXX

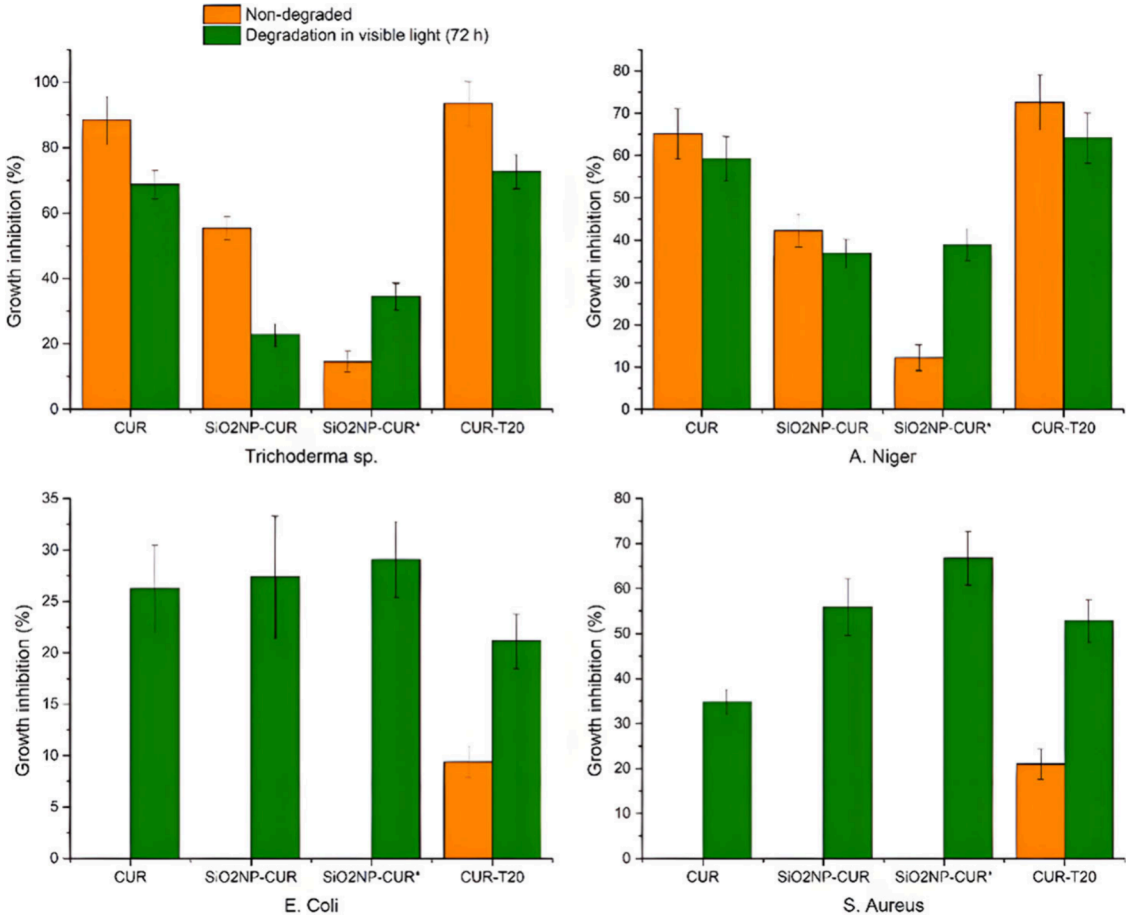

Figure 6. Inhibition of the growth of microorganisms. SiO_2NP-CUR* refers to only the material solubilized in water during the process.

Table 3 also shows that the charged silica-curcumin system degraded for 72 h showed lower antioxidant activity (0.0072 and 0.0076 mol g^{-1} for ABTS and DPPH, respectively) when compared to free curcumin degraded for 72 h (9.0197 and 8.2719 mol g^{-1}). From these results, we suggest that silica promoted the protection of curcumin, that is, it formed a slow-release silica-curcumin conjugate system. Furthermore, the loading of silica with curcumin in Tween 20 overcomes the barrier of low water solubility and the difficulties related to the delivery of these antioxidant compounds to specific sites in the human body. The silica-curcumin-Tween 20 slow delivery system opens perspectives on the use of this complex as an inexpensive and safe prodrug in the application of chronic disease therapies.[41]

3.6. Antimicrobial Potential of Curcumin. No sample was able to 100% inhibit the growth of microorganisms. However, photodegradation modified the antimicrobial profile of samples containing curcumin (Figure 6). The curcumin solution in water + Tween 20 was the sample with the greatest antimicrobial effect for both fungi, which was more pronounced against the fungus *Trichoderma* sp., which had its growth inhibited by 94 ± 7% in relation to the control. After anchoring in SiO_2NP, the microorganism was less susceptible to curcumin.

Photodegradation in visible light reduced the effect of curcumin on the growth of these microorganisms. It is known that the photodegradation of curcumin, as with other phenolic compounds, can lead to the generation of byproducts and reaction intermediates with biological activities different from their precursor during the reaction. This behavior depends on exposure variables, such as the wavelength, proximity of exposure to light, degradation kinetics, physical state of the compound, solvent used, and relative abundance of degradation products, among others.[44] Therefore, it is likely that the byproducts generated under the conditions tested here are less harmful than curcumin to the fungi used.

The results corroborate other studies that affirm the antifungal potential of curcumin against filamentous fungi. According to Zorofchian Moghadamtousi et al., this natural biocide acts on the regulation of the ERG3 gene, leading to a significant reduction in ergosterol in fungal cells.[45] The reduction in ergosterol production results in the accumulation of biosynthetic ergosterol precursors, which leads to cell death through the generation of ROS. It also acts on the development of hyphae, inhibiting their growth by targeting the global suppressor of thymidine uptake 1 (TUP1). The reduction in proteinase secretion and the change in membrane properties and ATPase activity are other possible factors for the antifungal activity of curcumin.

Interestingly, the antimicrobial potential of curcumin against bacteria was inverse to the potential obtained against filamentous fungi. It can be observed, under the conditions tested, that there was little or no activity of this biocide when in its natural form in aqueous conditions or under anchoring, but after the photodegradation reaction, the bacterial susceptibility to the samples was increased (Figure 6).

The Gram-positive bacterium *S. aureus* was more susceptible to curcumin than the Gram-negative bacterium *E. coli*. The

https://doi.org/10.1021/acsanm.4c05159
ACS Appl. Nano Mater. XXXX, XXX, XXX−XXX

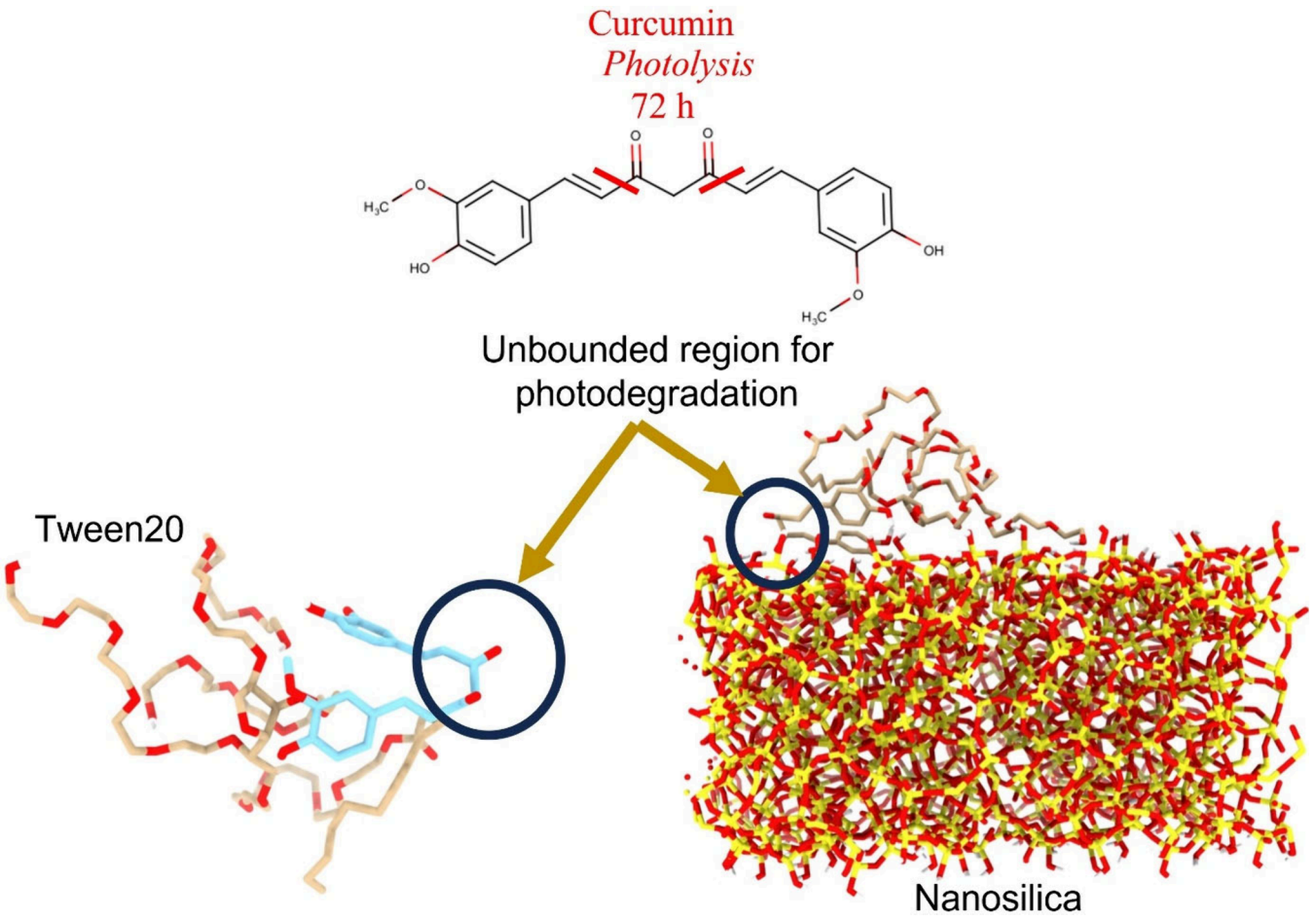

Figure 7. Docking studies of Tween 20 with curcumin and also with nanosilica. This is a qualitative indication that the region that undergoes photolysis can also be affected after anchoring with nanosilica and Tween 20.

best potential against *S. aureus* was obtained by the photodegraded anchored curcumin samples; 67 ± 6% inhibition of microbial growth was achieved when the sample was exposed to light.

Curcumin is a photosensitizer with phototoxicity and can act as a bactericide under blue light excitation.[46] The photobiological and photodynamic activities of curcumin are conferred by the formation of excited states and generation of singlet oxygen during photodegradation. Curcumin can be photoactivated by blue light (420−480 nm), which has limited tissue penetration. This feature makes curcumin as an antibacterial compound for oral or skin disinfection attractive, as it does not affect healthy tissue.[44] Curcumin can inhibit bacterial growth via disturbances in the cell membrane, cell wall, protein expression, damage to DNA and other cellular tissues, or through alterations in the quorum sensing (QS) system.[46] As an anti-infective agent, curcumin alters the bacterial QS system, not killing the bacteria themselves or destroying the mature biofilm but inhibiting the formation of that biofilm. Interacting with various molecular targets and transduction pathways, it modulates the biofilm and is also capable of reducing biofilm biomass and preventing its adhesion. Virulence factors that depend on QS are also inhibited. Therefore, curcumin may have beneficial synergistic effects with other antibacterial substances in combined treatments, increasing their efficiency, since the nonformation of the biofilm leaves the bacteria less resistant and consequently more susceptible to other drugs.[46]

The mechanism of action of photodegraded curcumin is related to its autoxidation and consequent formation of intermediate compounds, and as mentioned before, the profile of reactive intermediates can be modified by photodegradation. In agreement with what has been reported by other researchers,[45,46] the data obtained show that curcumin has potential for application as an antibacterial agent, especially against Gram-positive bacteria.

When curcumin is exposed to light, the incidence of light can induce an energy higher than the overall bond energy of intramolecular bonds. This can result in the disruption of the conjugated double bond system or, in the presence of organic solvents, lead to cleavage of the heptadiene chain.[47] Consequently, two major degradation pathways, namely solvolysis and oxidative degradation, can occur.[48] The photodegradation of curcumin generally leads to decomposition and the formation of five compounds: vanillin, ferulic aldehyde, ferulic acid, feruloylmethane, and bicyclopentadione.[49] Of particular interest, the bicyclopentadione derivative exhibits two oxygen atoms inserted into the heptadienedione chain that connects the phenolic rings.[50] Moreover, when curcumin is subjected to degradation in an aqueous buffer at physiological pH, autoxidation also takes place.[50−52] This process involves a radical chain reaction, resulting in the

https://doi.org/10.1021/acsanm.4c05159
ACS Appl. Nano Mater. XXXX, XXX, XXX−XXX

incorporation of oxygen into curcumin, ultimately forming the bicyclopentadione compound.

3.7. Docking Studies. In order to gain a better understanding of the effect of anchoring curcumin onto nanosilica, docking studies were conducted (Figure 7). The results, with and without nanosilica, revealed that the interaction of curcumin primarily occurs through its aryl side-chains.[48] Photolysis can take place in regions with weaker interactions among compounds, corresponding to the points of the weakest bonding. Consequently, this can lead to the formation of various derivative compounds and subsequent reactions. These findings help explain the antibacterial results, where even when anchored, these compounds can still form derivatives. However, further investigations are necessary to determine whether the observed effects are indeed due to the formation of radicals. This is because the interaction between nanosilica and Tween 20 may potentially disrupt these radicals compared with pure curcumin. Nevertheless, the notable results obtained suggest that nanosilica could potentially act as an antioxidant, as reported in a previous study.[53] Therefore, it can be considered that the intermediate products themselves might be the main contributing factor rather than the radicals alone.

4. CONCLUSIONS

The amorphization technique by anchoring onto nanoparticles can be successfully used for curcumin onto nanosilica by using Tween 20. The adsorption follows a BET model, with a more than 70% particle area reduction after loading, describing the chemical bonds occurring between the nanosilica and curcumin. This leads to an increase in thermal resistance for curcumin after loading, attributed to reactions between OH of curcumin and hydroxyls of the silica surface and complete amorphization, though still with low solubility. Therefore, the use of the photodegradation technique for curcumin performed in this work was effective in varying its chemical bonds in favor of curcumin bonds, leading to a small reduction in thermal degradation stability. However, due to the chemical compounds from photodegraded curcumin, there was an improvement in antioxidant capacity as well as its antibacterial properties. Therefore, these results corroborate that anchoring curcumin onto nanosilica improves the release rate and provides anchor points for photodegradation to occur with bound curcumin.

■ ASSOCIATED CONTENT

Supporting Information

The Supporting Information is available free of charge at https://pubs.acs.org/doi/10.1021/acsanm.4c05159.

Scanning electron microscopy images of pure curcumin and anchored SiO_2NP-CUR (PDF)

■ AUTHOR INFORMATION

Corresponding Authors

Gabriel Goetten de Lima − *Materials Research Institute, Technological University of the Shannon, Athlone, Ireland N37 HD68;* orcid.org/0000-0002-6161-4626; Phone: +353 (0)90 646 8000; Email: ggoetten@research.ait.ie

Pedro Henrique Gonzalez de Cademartori − *Graduate Program in Engineering & Materials Science (PIPE), Federal University of Paraná (UFPR), Polytechnic Center,, Curitiba 81531-990, Brazil;* orcid.org/0000-0003-3295-6907; Phone: +55 (41) 996951039; Email: pedroc@ufpr.br

Authors

Luana Nunes dos Santos Quelé − *EMBRAPA Florestas, 83411-000 Colombo, Paraná, Brazil*

Mauricio de Matos − *SENAI Innovation Institute for Electrochemistry, 81920-380 Curitiba, Paraná, Brazil*

Tatiane Brugnari − *Graduate Program in Engineering & Materials Science (PIPE), Federal University of Paraná (UFPR), Polytechnic Center,, Curitiba 81531-990, Brazil*

Carolina Simões Pires Ribeiro − *Graduate Program in Engineering & Materials Science (PIPE), Federal University of Paraná (UFPR), Polytechnic Center,, Curitiba 81531-990, Brazil*

Alessandra Cristina Pedro − *EMBRAPA Florestas, 83411-000 Colombo, Paraná, Brazil*

Washington Luiz Esteves Magalhães − *EMBRAPA Florestas, 83411-000 Colombo, Paraná, Brazil;* orcid.org/0000-0003-4405-293X

Complete contact information is available at: https://pubs.acs.org/10.1021/acsanm.4c05159

Author Contributions

The manuscript was written through contributions of all authors. All authors have given approval to the final version of the manuscript.

Funding

This study was financed in part by the Coordenação de Aperfeiçoamento de Pessoal de Nivel Superior - Brasil (CAPES) - Finance Code 001. The Article Processing Charge for the publication of this research was funded by the Coordination for the Improvement of Higher Education Personnel - CAPES (ROR identifier: 00x0ma614).

Notes

The authors declare no competing financial interest.

■ REFERENCES

(1) El-Saadony, M. T.; Yang, T.; Korma, S. A.; Sitohy, M.; Abd El-Mageed, T. A.; Selim, S.; Al Jaouni, S. K.; Salem, H. M.; Mahmmod, Y.; Soliman, S. M.; Mo'men, S. A. A.; Mosa, W. F. A.; El-Wafai, N. A.; Abou-Aly, H. E.; Sitohy, B.; Abd El-Hack, M. E.; El-Tarabily, K. A.; Saad, A. M. Impacts of Turmeric and Its Principal Bioactive Curcumin on Human Health: Pharmaceutical, Medicinal, and Food Applications: A Comprehensive Review. *Front Nutr* **2023**, *9*, No. 1040259.

(2) Salehi, B.; Rodrigues, C. F.; Peron, G.; Dall'Acqua, S.; Sharifi-Rad, J.; Azmi, L.; Shukla, I.; Singh Baghel, U.; Prakash Mishra, A.; Elissawy, A. M.; Singab, A. N.; Pezzani, R.; Redaelli, M.; Patra, J. K.; Kulandaisamy Venil, C.; Das, G.; Singh, D.; Kriplani, P.; Venditti, A.; Fokou, P. V. T.; Iriti, M.; Amarowicz, R.; Martorell, M.; Cruz-Martins, N. Curcumin Nanoformulations for Antimicrobial and Wound Healing Purposes. *Phytotherapy Research* **2021**, *35* (5), 2487−2499.

(3) Chagas, P. A. M.; Schneider, R.; dos Santos, D. M.; Otuka, A. J. G.; Mendonça, C. R.; Correa, D. S. Bilayered Electrospun Membranes Composed of Poly(Lactic-Acid)/Natural Rubber: A Strategy against Curcumin Photodegradation for Wound Dressing Application. *React. Funct Polym.* **2021**, *163*, No. 104889.

(4) Kong, Z.-L.; Kuo, H.-P.; Johnson, A.; Wu, L.-C.; Chang, K. L. B. Curcumin-Loaded Mesoporous Silica Nanoparticles Markedly Enhanced Cytotoxicity in Hepatocellular Carcinoma Cells. *Int. J. Mol. Sci.* **2019**, *20* (12), 2918.

(5) DENG, Y.; VERRON, E.; ROHANIZADEH, R. Molecular Mechanisms of Anti-Metastatic Activity of Curcumin. *Anticancer Res.* **2016**, *36* (11), 5639−5648.

(6) Jung, Y. N.; Hong, J. Changes in Chemical Properties and Bioactivities of Turmeric Pigments by Photo-Degradation. *AIMS Agriculture and Food* **2021**, *6* (2), 754−767.
(7) Jung, Y. N.; Hong, J. Changes in Chemical Properties and Bioactivities of Turmeric Pigments by Photo-Degradation. *AIMS Agriculture and Food* **2021**, *6* (2), 754−767.
(8) Roy, S.; Priyadarshi, R.; Ezati, P.; Rhim, J.-W. Curcumin and Its Uses in Active and Smart Food Packaging Applications - a Comprehensive Review. *Food Chem.* **2022**, *375*, No. 131885.
(9) Ansari, L.; Mashayekhi-Sardoo, H.; Baradaran Rahimi, V.; Yahyazadeh, R.; Ghayour-Mobarhan, M.; Askari, V. R. Curcumin-based Nanoformulations Alleviate Wounds and Related Disorders: A Comprehensive Review. *BioFactors* **2023**, *49* (4), 736−781.
(10) Le, K. M.; Trinh, N.-T.; Nguyen, V. D.-X.; Van Nguyen, T.-D.; Thi Nguyen, T.-H.; Van Vo, T.; Tran, T. Q.; Ngo, D.-N.; Vong, L. B. Investigating the Anti-Inflammatory Activity of Curcumin-Loaded Silica-Containing Redox Nanoparticles. *J. Nanomater* **2021**, *2021*, 1−11.
(11) Slika, L.; Patra, D. A Short Review on Chemical Properties, Stability and Nano-Technological Advances for Curcumin Delivery. *Expert Opin Drug Deliv* **2020**, *17* (1), 61−75.
(12) Mahesh, T.; Balasubashini, M. S.; Menon, V. P. Effect of Photo-Irradiated Curcumin Treatment Against Oxidative Stress in Streptozotocin-Induced Diabetic Rats. *Journal of Medicinal Food* **2005**, *8* (2), 251−255.
(13) Mattos, B. D.; Tardy, B. L.; Pezhman, M.; Kämäräinen, T.; Linder, M.; Schreiner, W. H.; Magalhães, W. L. E.; Rojas, O. J. Controlled Biocide Release from Hierarchically-Structured Biogenic Silica: Surface Chemistry to Tune Release Rate and Responsiveness. *Sci. Rep.* **2018**, *8* (1), 5555.
(14) Yuh-Shan, H. Citation Review of Lagergren Kinetic Rate Equation on Adsorption Reactions. *Scientometrics* **2004**, *59* (1), 171−177.
(15) Ho, Y. S.; McKay, G. Sorption of Dye from Aqueous Solution by Peat. *Chemical Engineering Journal* **1998**, *70* (2), 115−124.
(16) Wu, F.-C.; Tseng, R.-L.; Juang, R.-S. Characteristics of Elovich Equation Used for the Analysis of Adsorption Kinetics in Dye-Chitosan Systems. *Chemical Engineering Journal* **2009**, *150* (2−3), 366−373.
(17) Langmuir, I. THE ADSORPTION OF GASES ON PLANE SURFACES OF GLASS, MICA AND PLATINUM. *J. Am. Chem. Soc.* **1918**, *40* (9), 1361−1403.
(18) Freundlich, H. M. F. Over the Adsorption in Solution. *J. Phys. Chem* **1906**, *57*, 1100−1107.
(19) Wang, J.; Huang, C. P.; Allen, H. E.; Cha, D. K.; Kim, D.-W. Adsorption Characteristics of Dye onto Sludge Particulates. *J. Colloid Interface Sci.* **1998**, *208* (2), 518−528.
(20) Re, R.; Pellegrini, N.; Proteggente, A.; Pannala, A.; Yang, M.; Rice-Evans, C. Antioxidant Activity Applying an Improved ABTS Radical Cation Decolorization Assay. *Free Radical Biol. Med.* **1999**, *26* (9−10), 1231−1237.
(21) Rufino, M. d. S. M.; Alves, R. E.; de Brito, E. S.; de Morais, S. M.; Sampaio, C. d. G.; Pérez-Jiménez, J.; Saura-Calixto, F. D. In *Metodologia Científica: Determinação Da Atividade Antioxidante Total Em Frutas Pela Captura Do Radical Livre DPPH*; Embrapa Agroindústria Tropical, 2007.
(22) Brand-Williams, W.; Cuvelier, M. E.; Berset, C. Use of a Free Radical Method to Evaluate Antioxidant Activity. *LWT - Food Science and Technology* **1995**, *28* (1), 25−30.
(23) Stewart, J. J. P. MOPAC: A Semiempirical Molecular Orbital Program. *Journal of Computer-Aided Molecular Design* **1990**, *4* (1), 1−103.
(24) Emami, F. S.; Puddu, V.; Berry, R. J.; Varshney, V.; Patwardhan, S. V.; Perry, C. C.; Heinz, H. Force Field and a Surface Model Database for Silica to Simulate Interfacial Properties in Atomic Resolution. *Chem. Mater.* **2014**, *26* (8), 2647−2658.
(25) Morris, G. M.; Huey, R.; Lindstrom, W.; Sanner, M. F.; Belew, R. K.; Goodsell, D. S.; Olson, A. J. AutoDock4 and AutoDockTools4: Automated Docking with Selective Receptor Flexibility. *J. Comput. Chem.* **2009**, *30* (16), 2785−2791.
(26) Dolinsky, T. J.; Nielsen, J. E.; McCammon, J. A.; Baker, N. A. PDB2PQR: An Automated Pipeline for the Setup of Poisson-Boltzmann Electrostatics Calculations. *Nucleic Acids Res.* **2004**, *32*, W665−W667.
(27) Ritchie, D. W.; Kozakov, D.; Vajda, S. Accelerating and Focusing Protein−Protein Docking Correlations Using Multi-Dimensional Rotational FFT Generating Functions. *Bioinformatics* **2008**, *24* (17), 1865−1873.
(28) Goetten de Lima, G.; Wilke Sivek, T.; Matos, M.; Lundgren Thá, E.; de Oliveira, K. M. G.; Rodrigues de Souza, I.; de Morais de Lima, T. A.; Cestari, M. M.; Esteves Magalhães, W. L.; Hansel, F. A.; Morais Leme, D. A Biocide Delivery System Composed of Nanosilica Loaded with Neem Oil Is Effective in Reducing Plant Toxicity of This Biocide. *Environ. Pollut.* **2022**, *294*, No. 118660.
(29) Zou, L.; Zheng, B.; Zhang, R.; Zhang, Z.; Liu, W.; Liu, C.; Zhang, G.; Xiao, H.; McClements, D. J. Influence of Lipid Phase Composition of Excipient Emulsions on Curcumin Solubility, Stability, and Bioaccessibility. *Food Biophysics* **2016**, *11* (3), 213−225.
(30) Wang, M. C.; Sheng, G. D.; Qiu, Y. P. A Novel Manganese-Oxide/Biochar Composite for Efficient Removal of Lead(II) from Aqueous Solutions. *International Journal of Environmental Science and Technology* **2015**, *12* (5), 1719−1726.
(31) Bullen, J. C.; Saleesongsom, S.; Gallagher, K.; Weiss, D. J. A Revised Pseudo-Second-Order Kinetic Model for Adsorption, Sensitive to Changes in Adsorbate and Adsorbent Concentrations. *Langmuir* **2021**, *37* (10), 3189−3201.
(32) Giles, C. H.; Smith, D.; Huitson, A. A General Treatment and Classification of the Solute Adsorption Isotherm. I. Theoretical. *J. Colloid Interface Sci.* **1974**, *47* (3), 755−765.
(33) Tran, H. N.; You, S.-J.; Hosseini-Bandegharaei, A.; Chao, H.-P. Mistakes and Inconsistencies Regarding Adsorption of Contaminants from Aqueous Solutions: A Critical Review. *Water Res.* **2017**, *120*, 88−116.
(34) Yahia, M. B.; Wjihi, S. Study of the Hydrogen Physisorption on Adsorbents Based on Activated Carbon by Means of Statistical Physics Formalism: Modeling Analysis and Thermodynamics Investigation. *Sci. Rep* **2020**, *10*, 16118.
(35) Xu, L.; Zhang, J.; Ding, J.; Liu, T.; Shi, G.; Li, X.; Dang, W.; Cheng, Y.; Guo, R. Pore Structure and Fractal Characteristics of Different Shale Lithofacies in the Dalong Formation in the Western Area of the Lower Yangtze Platform. *Minerals* **2020**, *10* (1), 72.
(36) Goetten de Lima, G.; Wilke Sivek, T.; Matos, M.; Lundgren Thá, E.; de Oliveira, K. M. G.; Rodrigues de Souza, I.; de Morais de Lima, T. A.; Cestari, M. M.; Esteves Magalhães, W. L.; Hansel, F. A.; Morais Leme, D. A Biocide Delivery System Composed of Nanosilica Loaded with Neem Oil Is Effective in Reducing Plant Toxicity of This Biocide. *Environ. Pollut.* **2022**, *294*, No. 118660.
(37) Sreeharsha, N.; Philip, M.; Krishna, S. S.; Viswanad, V.; Sahu, R. K.; Shiroorkar, P. N.; Aasif, A. H.; Fattepur, S.; Asdaq, S. M. B.; Nair, A. B.; Attimarad, M.; Venugopala, K. N. Multifunctional Mesoporous Silica Nanoparticles for Oral Drug Delivery. *Coatings* **2022**, *12* (3), 358.
(38) Yadav, Y. C.; Pattnaik, S.; Swain, K. Curcumin Loaded Mesoporous Silica Nanoparticles: Assessment of Bioavailability and Cardioprotective Effect. *Drug Dev. Ind. Pharm.* **2019**, *45* (12), 1889−1895.
(39) He, Y.; Yue, Y.; Zheng, X.; Zhang, K.; Chen, S.; Du, Z. Curcumin, Inflammation, and Chronic Diseases: How Are They Linked? *Molecules* **2015**, *20* (5), 9183−9213.
(40) Tai, K.; Rappolt, M.; Mao, L.; Gao, Y.; Li, X.; Yuan, F. The Stabilization and Release Performances of Curcumin-Loaded Liposomes Coated by High and Low Molecular Weight Chitosan. *Food Hydrocolloids* **2020**, *99*, No. 105355.
(41) Jung, Y. N.; Hong, J. Changes in Chemical Properties and Bioactivities of Turmeric Pigments by Photo-Degradation. *AIMS Agriculture and Food* **2021**, *6* (2), 754−767.

https://doi.org/10.1021/acsanm.4c05159
ACS Appl. Nano Mater. XXXX, XXX, XXX−XXX

(42) Wang, Y.-J.; Pan, M.-H.; Cheng, A.-L.; Lin, L.-I.; Ho, Y.-S.; Hsieh, C.-Y.; Lin, J.-K. Stability of Curcumin in Buffer Solutions and Characterization of Its Degradation Products. *J. Pharm. Biomed. Anal.* **1997**, *15* (12), 1867−1876.
(43) Jung, Y. N.; Kang, S.; Lee, B. H.; Kim, J. H.; Hong, J. Changes in the Chemical Properties and Anti-Oxidant Activities of Curcumin by Microwave Radiation. *Food Science and Biotechnology* **2016**, *25* (5), 1449−1455.
(44) JANKUN, J.; WYGANOWSKA-ŚWIĄTKOWSKA, M.; DETTLAFF, K.; JELIŃSKA, A.; SURDACKA, A.; WĄTRÓBSKA-ŚWIETLIKOWSKA, D.; SKRZYPCZAK-JANKUN, E. Determining Whether Curcumin Degradation/Condensation Is Actually Bioactivation (Review). *Int. J. Mol. Med.* **2016**, *37* (5), 1151−1158.
(45) Zorofchian Moghadamtousi, S.; Abdul Kadir, H.; Hassandarvish, P.; Tajik, H.; Abubakar, S.; Zandi, K. A Review on Antibacterial, Antiviral, and Antifungal Activity of Curcumin. *BioMed. Research International* **2014**, *2014*, 1−12.
(46) Zheng, D.; Huang, C.; Huang, H.; Zhao, Y.; Khan, M. R. U.; Zhao, H.; Huang, L. Antibacterial Mechanism of Curcumin: A Review. *Chemistry & Biodiversity* **2020**, *17* (8), e2000171 DOI: 10.1002/cbdv.202000171.
(47) Schneider, C. Understanding the Misunderstood: Products and Mechanisms of the Degradation of Curcumin. In *Recent Advances in Polyphenol Research*; John Wiley & Sons, Ltd., Chichester, UK, 2019; p 335−361. DOI: 10.1002/9781119427896.ch12.
(48) Nelson, K. M.; Dahlin, J. L.; Bisson, J.; Graham, J.; Pauli, G. F.; Walters, M. A. The Essential Medicinal Chemistry of Curcumin. *J. Med. Chem.* **2017**, *60* (5), 1620−1637.
(49) Appendino, G.; Allegrini, P.; de Combarieu, E.; Novicelli, F.; Ramaschi, G.; Sardone, N. Shedding Light on Curcumin Stability. *Fitoterapia* **2022**, *156*, No. 105084.
(50) Gordon, O. N.; Luis, P. B.; Sintim, H. O.; Schneider, C. Unraveling Curcumin Degradation. *J. Biol. Chem.* **2015**, *290* (8), 4817−4828.
(51) Tønnesen, H. H.; Másson, M.; Loftsson, T. Studies of Curcumin and Curcuminoids. XXVII. Cyclodextrin Complexation: Solubility, Chemical and Photochemical Stability. *Int. J. Pharm.* **2002**, *244*, 127−135.
(52) Gordon, O. N.; Schneider, C. Vanillin and Ferulic Acid: Not the Major Degradation Products of Curcumin. *Trends in Molecular Medicine* **2012**, *18* (7), 361−363.
(53) Gao, X.; Meng, X.; Wang, H.; Wen, B.; Ding, Y.; Zhang, S.; Yang, M. Antioxidant Behaviour of a Nanosilica-Immobilized Antioxidant in Polypropylene. *Polym. Degrad. Stab.* **2008**, *93* (8), 1467−1471.

https://doi.org/10.1021/acsanm.4c05159
ACS Appl. Nano Mater. XXXX, XXX, XXX−XXX